Influence of Process Interactions on MJO-like Convective Structures in the IFS Model

Adrian Tompkins and Thomas Jung

ECMWF, Shinfield Park, Reading
RG2 9AX, United Kingdom
tompkins@ecmwf.int, jung@ecmwf.int

ABSTRACT

This project had two main objectives: To document some basic diagnostics of tropical, eastward propagating, MJO-like modes in the ECMWF model, and then to investigate the sensitivity of these modes to various process interactions, such as the feedback between water vapour and deep convection.

The first task identified a distinct east propagating feature in the lower and upper level zonal wind and 200 hPa velocity potential at wavenumber 1. Unlike for the observations, however, no distinct spectral peak is found in the frequency domain for the IFS. Moreover, wavenumber 1 features in the IFS propagate eastward at a speed of about 19 m s^{-1}, that is, much faster than what is known from the observations. More analysis is required, but it is likely that the mode represents moist convectively-coupled Kelvin wave activity. A significant contrast was noted between the T95 resolution model, used for seasonal forecasting, and higher resolutions such as the T159 model used for the monthly forecast, and the operational T511 model. The higher resolution models appear to significantly damp the low wavenumber modes with respect to analysis data.

The physics of the default model was then modified in a number of ways in an attempt to suppress or exacerbate the feedback between convection and water vapour and examine the consequence for the eastward propagating mode. Apparently the power in the eastward propagating mode was quite sensitive to the attempts to alter this feedback. However, further investigation led to an unsatisfying, but robust conclusion. This is namely that the zero-order effect of the model alterations were simply to suppress or enhance the amount of parameterized deep convection, altering the balance between the large-scale and parameterized latent heating. Increasing the proportion of parameterized convection damps the eastward propagating mode. We proffer a hypothesis as to why this may be the case, and suggest that it is likely that some additional mechanism such as convective-water vapour feedback is required to produce the slower MJO mode, which is currently lacking from the model.

This investigation highlights the danger of jumping to 'physically-based' conclusions when working with complex numerical models. It is always tempting to associate model behaviour with mechanisms that one can imagine applying in nature, while in fact numerical artifacts can be dominating a response. The study also highlights some characteristics of parameterized convection that can be further investigated, such as its relation to large-scale motions for example.

1 Introduction

The significant contribution of the Madden-Julian Oscillation (MJO) (Madden and Julian, 1971, 1972) to Tropical intraseasonal variability renders it an important feature to simulate successfully in climate and forecast models. The initial aim of this work is to briefly document the MJO activity in the ECMWF Integrated Forecast System (IFS) model. This is important given that no documentation of the MJO as simulated by the IFS has been conducted since the study of Slingo et al. (1996), while the model has evolved considerably in the meantime.

In addition to dynamical mechanisms such as wave-CISK (Hayashi, 1970), wind induced heat exchange (WISHE) (Emanuel, 1987; Neelin et al., 1987) and lateral forcing from mid-latitudes (Zhang and Webster, 1992) (see Hayashi and Golder (1997) for complete review), more recently attention has additionally focused on the role

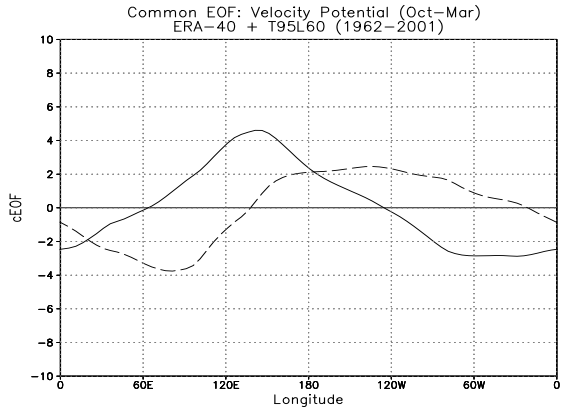

Figure 1: First (solid) and second (dashed) EOF of wintertime (Oct–Mar) tropical velocity potential anomalies ($m^2 s^{-1}$) based on the period 1962–2001 and the combined ERA-40 reanalysis and T_L95L60 model dataset.

that thermodynamic feedbacks could play in regulating the strength and propagation characteristics of simulated MJO. These have included feedbacks with sea surface temperature (SST) anomalies (Hendon, 2000; Woolnough et al., 2001; Inness and Slingo, 2003), cloud-radiation interaction (Raymond, 2001; Lee et al., 2001), and water vapour-convective feedback (Bladé and Hartmann, 1993; Tompkins, 2001; Inness et al., 2001; Grabowski, 2003).

The second aim was to examine some of these thermodynamic feedbacks to determine what role, if any, they played in propagating modes of convection. Here, we report only the results of experiments conducted chiefly to investigate the role of water vapour and its interaction with deep convection.

2 The MJO in the IFS

2.1 The MJO in seasonal integrations

In this section the performance of the ECMWF forecast model in simulating the MJO is described by diagnosing six month seasonal integrations starting on 1st October (extended winter season) for the period 1962–2001. The summer season is omitted here for brevity. Details on the performance of the ECMWF model during summertime are very similar and described elsewhere (Jung and Tompkins, 2003). Unless stated otherwise, all seasonal forecast results are based on model cycle 26r1 with a resolution of T_L95L60. This cycle was operational at ECMWF from 14 January to 7 October 2003.

In this study the velocity potential at pressure level 200hPa (VPOT, hereafter) is used to identify MJO-like activity. At this level VPOT, describes the large-scale divergent part of the upper-tropospheric flow. The focus is on the Tropics. To this end VPOT fields have been averaged from 5^oS to 5^oN. Daily data were smoothed by forming 4 day non-overlapping averages. Thus, each extended season consists of a total of 46 4-day mean fields. Finally, prior to diagnosis, the mean annual cycle has been removed.

The first two Empirical Orthogonal Functions (EOFs) of wintertime tropical VPOT anomalies are shown in Fig. 1 for the combined ERA-40 and model dataset. Note, that the first 46 by 40 vectors of the combined dataset are ERA-40 anomalies and the last 46 by 40 vectors are formed by simulated anomalies. By performing EOF analysis for the combined data set principal axes can be found that are *common* to both datasets. For this reason we shall call this technique common EOF analysis (cEOF analysis) hereafter (Barnett et al., 1999, for details see). The first and second cEOFs explain 35.6% and 26.4% of the total tropical VPOT variance. The first two EOFs show wavenumber one type structures which are reminiscent of the MJO. The first EOF

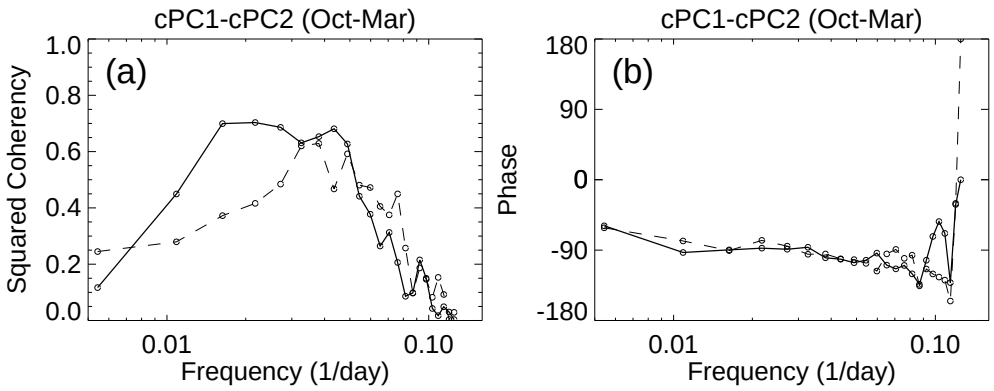

Figure 2: (a) Squared coherency and (b) phase spectrum for the first two common PCs of wintertime tropical velocity potential anomalies from ERA-40 data. Smoothing has been performed by averaging over all 40 winters (i.e., equivalent degrees of freedom amount to 80). The squared coherency spectrum shows how different frequencies contribute to the squared correlation coefficient. The first PC leads the second PC in (b) for negative phases. Methodological details can be found, for example, in Jenkins and Watts (1968).

describes out-of-phase anomalies between the warm pool and the tropical Atlantic, whereas the second EOF shows anomalies of opposite polarity over the Indian and Pacific ocean. The first two EOFs are clearly in quadrature.

As noted above, the MJO can be characterized by tropical VPOT anomalies of wavenumber one. Moreover, these anomalies tend to propagate eastward. Therefore, for the MJO to be efficiently described by the leading two EOFs, the first two principal components (PCs, hereafter) should be in quadrature—with PC1 leading PC2 by 90^o. The squared coherency and phase spectrum between the first two cPCs are shown in Fig. 2 for the ERA-40 (solid) and model (dashed) data. The cPCs were obtained by separately projecting observed and modelled anomalies onto the leading two cEOFs. Significant squared coherency between the leading two cPCs is found for ERA-40 data on timescales from 20–60 days. Furthermore, cPC1 leads cPC2 by about 90^o confirming that the leading two cEOFs describe MJO variability. For the ECWMF model, however, significant squared coherency is evident on timescales from 20–30 days only, that is, the leading two cPCs are much less coherent than the observations on time scales longer than 30 days. This confirms previous (subjective) experience with the ECWMF model that the model underestimates MJO-related *slowly* eastward propagating VPOT anomalies.

Next, the model's capability to simulate the strength of MJO-like variability is investigated. To this end partial eigenvalues (pEVs) were computed for each of the two datasets and every winter during the period 1962–2001 (Fig. 3). The pEVs were obtained by projecting VPOT anomalies for every winter onto the normalized leading cEOFs and by computing the variance of the projection coefficients (cPCs) for each winter separately. Thus, high (low) values suggest high (low) activity along the direction of the respective cEOF. Firstly, it is evident that activity in the eastward propagating mode, as given by the pEVs for the first two cEOFs, shows pronounced interannual variability. In fact individual pEVs for the first two eigenmodes differ by as much as a factor of 4 between individual years. This clearly shows that relatively long time series are necessary in order to draw meaningful conclusions of the model's capability to simulate MJO activity. Average pEVs are shown in Fig. 3b along with 95% confidence levels. From these statistics it is evident that MJO activity in the ECWMF model is underestimated by about 10% compared to the analyses, and that the model overestimates activity along the direction of cEOF mode 2–10 (These modes describe VPOT variability at higher wavenumbers).

The spectral characteristics of the observed and modelled MJO are studied. Average power spectra and 95% confidence intervals are shown in Fig. 4 for the first two cPCs based on ERA-40 data (solid) and the 6 month model integrations (dashed). The observed MJO clearly shows a broad-band peak on intraseasonal time scales (30–60 days). In contrast, the model spectra show no broad-band peaks; they rather resemble those of first-order auto-regressive processes. The underestimation of MJO variability of the model is particularly pronounced (and

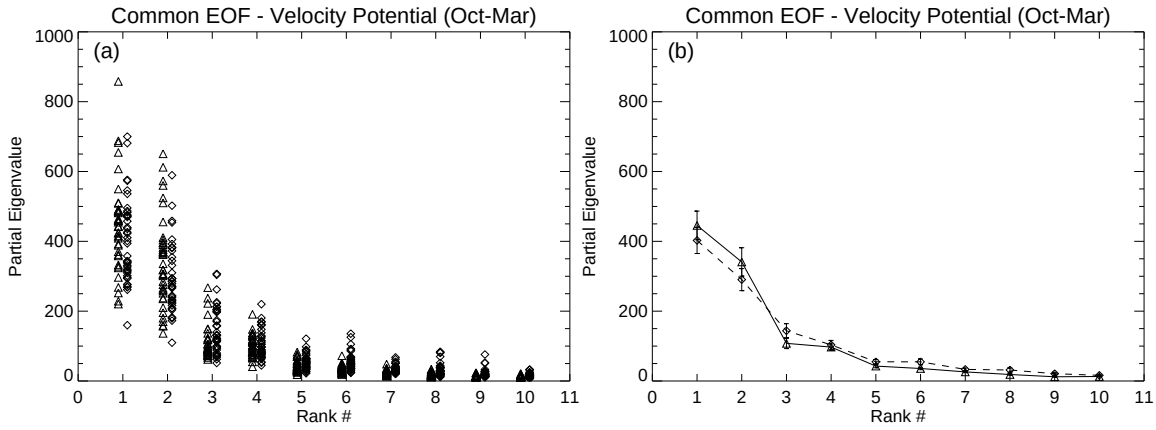

Figure 3: (a) Partial eigenvalues for ERA-40 reanalysis data (triangles) and T_L95L60 integrations based on model cycle 26r1 (diamonds) for the leading 10 common EOF modes of wintertime (Oct–Mar) tropical velocity potential anomalies (m^2s^{-1}) based on the period 1962–2001. For each winter one triangle (diamond) is shown. (b) Average and 95% confidence intervals for the partial eigenvalues shown in (a).

statistically significant) on longer timescales (i.e., around 60 days.)

Finally, we discuss the sensitivity of the eastward propagating mode to changes in the horizontal resolution. While studying the capability of the ECMWF model to simulate the MJO during the first 30 days of the integration, Vitart et al. (2003) found that MJO variance decreases during the first 10 days by as much as 50%. This is contrast to the model integrations described above, where the loss in variance amounts to only about 10%. There are several possible reasons for these differences. Monthly forecasts are based on a coupled atmosphere-ocean model and the drift of the coupled model system might deteriorate the MJO. Furthermore, most of the monthly forecasts were performed at a different horizontal (T_L159) and vertical (L40) resolution using older model cycles. Therefore, it might well be possible that the MJO is sensitive to coupled model drift, resolution or model formulation (model cycles).

In order to test the sensitivity to horizontal resolution, six-month integrations for the summer and winter seasons of the years 1991–1998 have been performed using model cycle 25r1[1] at two different resolutions (T_L95L60

[1]The integrations with model cycle 25r1 formed a pilot study to ascertain the choice of horizontal resolution to use for the full study

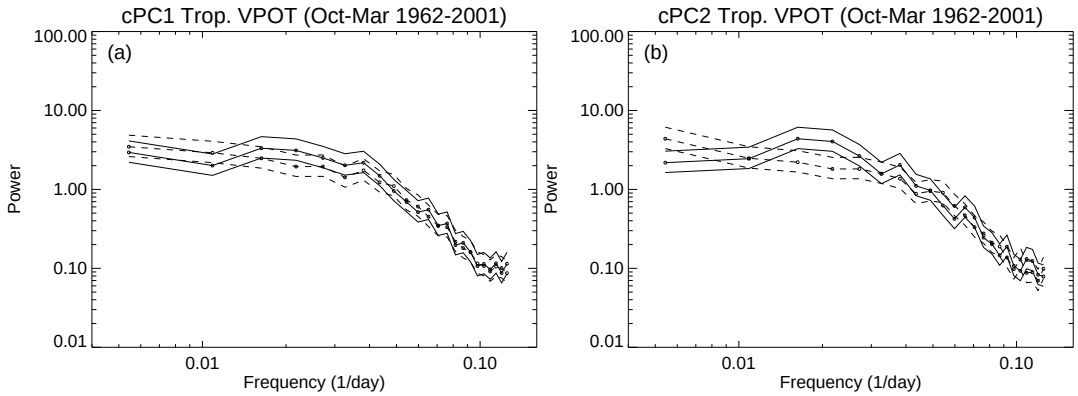

Figure 4: Smoothed power spectrum of the (a) first and (b) second PC of wintertime tropical velocity potential anomalies based on ERA-40 data (solid) and T_L95L60 integrations based on model cycle 26r1 (dashed). Thin lines denote 95% confidence levels. Details on the method are given, for example, by von Storch and Zwiers (1999).

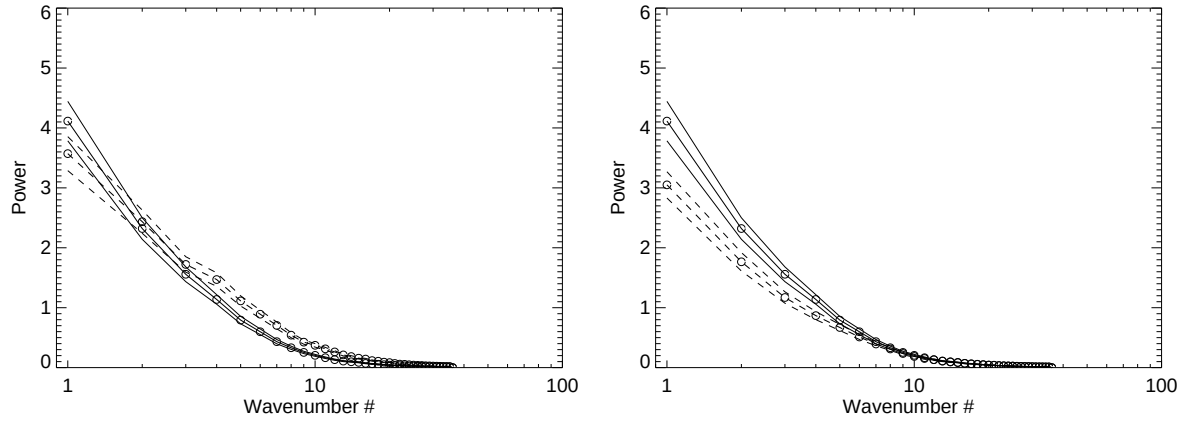

Figure 5: Analysed (solid) and simulated (dashed) wavenumber spectra for wintertime tropical VPOT anomalies: (left) T_L95L60 and (right) T_L159L60. Also shown are 95% confidence intervals. Results are based on 6 months integrations over the period 1991–98 based on model cycle 25r1.

versus T_L159L60). Average wavenumber spectra of summertime tropical VPOT anomalies from ERA-40 and the ECMWF model are shown in Fig. 5 for the T_L95L60 (left) and the T_L159L60 (right) model. Results for the winter season are very similar (not shown). Consistent with the results for the Monthly Forecasting system the relatively high-resolution (T_L159L60) model underestimates wavenumber 1 variance by about 30%. The lower-resolution model (T_L95L60), on the other hand, shows much more realistic values of variance at wavenumber one. This result clearly indicates a large sensitivity of wavenumber 1 variance with respect to horizontal resolution.

2.2 The MJO in medium-range forecasts

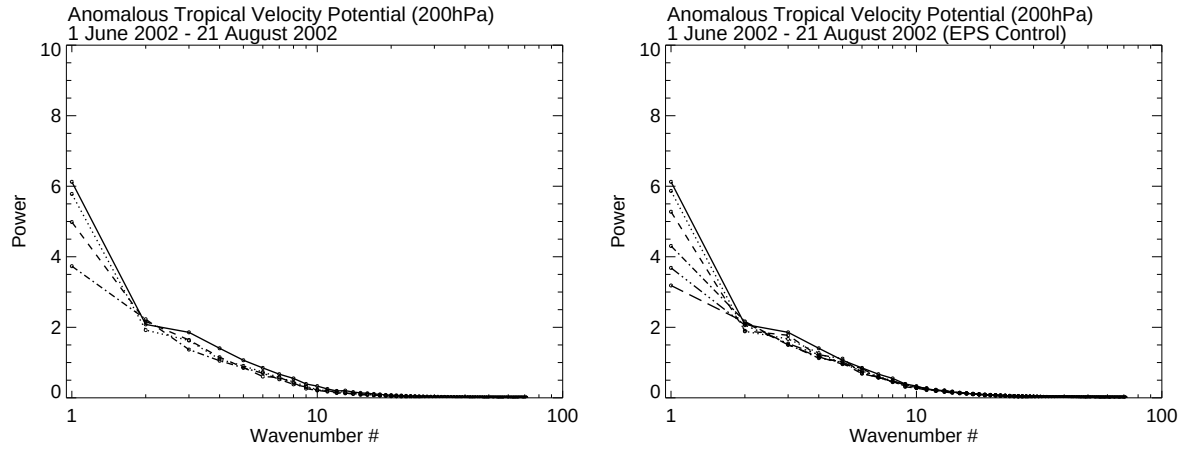

Figure 6: Wavenumber spectra of tropical VPOT anomalies for (left) operational high-resolution deterministic (T_L511L60) and (right) EPS control forecasts (T_L255L40). Shown are estimates based on D+0 (solid, analysis), D+2 (dotted), D+5 (dashed), D+10 (dash-dotted), D+15 (dash-dot-dot-dot), and D+20 (long-dashed) forecasts. Results are for the summer period 1 June 2002 to 21 August 2002.

As shown in the previous section the T_L159L60 model shows a larger loss of MJO variance than the T_L95L60 (30% versus 10%). It is interesting to address the question whether models at horizontal resolutions higher

with model cycle 26r1.

than T_L159 show a similar behaviour as the $T_L159L60$ model. To this end operational medium-range forecasts at $T_L255L60$ (EPS control) and $T_L511L60$ (deterministic forecast) of tropical VPOT anomalies were diagnosed. Average wavenumber spectra of tropical VPOT anomalies for the period 1 June 2002 to 21 August 2002 are shown in Fig. 6 for the operational analysis (solid) and deterministic (left) as well as EPS control (right) forecasts. At both resolutions a large loss of MJO-type variance can be found during the first 10 days of the integration (about 30 %). The EPS control forecasts show that this loss of variance continues into the near extended-range (10–20 days) where the simulated variance amounts to about 50% of the values for the analyses.

3 Sensitivity tests

It has been established that the chief eastward propagating wavenumber 1 feature in the ECMWF IFS model is too fast compared to the observations. Further analysis is required but the mode appears to resemble a convectively coupled moist Kelvin wave. The mode is present in a variety of model resolutions.

The introduction outlined some suggested thermodynamics feedback that could play a role in the propagation of the MJO in nature, including the feedback between deep convection and water vapour. This mechanism is based on the fact that convection moistens the troposphere locally. Moist air is more favourable for future convection, since the entrainment of dry air into updraughts significantly reduces their buoyancy. Additionally, a drier mid-troposphere will drive stronger downdraughts, lowering the boundary layer moist static energy, and reducing the possibility of future convection. Therefore the action of convective moistening effectively 'preconditions' the environment for future deep convective activity. The suggestion of a feedback existing between convection and water vapour is not recent, and has a basis in earlier convective observations and modelling studies (Esbensen, 1978; LeMone and Zipser, 1980; Nicholls and Lemone, 1980; Randall and Huffman, 1980). The recent development has been to extend this mechanism to cases of deep convective organisation in low wind shears (Tompkins, 2001). The suggested role played in the MJO is that the time taken to precondition the atmosphere by shallow and subsequently deep convection slows down the propagating convective modes.

A set of sensitivity tests intended to either enhance or suppress this water vapour feedback has been designed. A summary of the tests is provided in Table 1. One experiment in which a prognostic memory for convection is introduced, does not specifically examine the water vapour role and is included to provide a benchmark sensitivity. In order to reduce the numerical cost to permit the wider range of tests, the experiments are conducted using an 'aqua planet' setup, where the surface is zonal symmetric ocean with the temperature specified by the control case of Neale and Hoskins (2000). Perpetual July radiative conditions are applied. The integrations are conducted for one year, although a number of experiments are duplicated for a second year to estimate the influence of sampling variability.

Only three experiments will be discussed here. The first pair of experiments attempt to isolate the link between convection and boundary layer moist static energy through the action of precipitation evaporation. Grabowski and Moncrieff (2004) found a strong sensitivity to the rainfall fall evaporation using the Emanuel (1991) convection scheme. Unlike the Emanuel scheme, the current Tiedtke (1989) implementation only allows for convective precipitation evaporation in the subcloud layer. We enhance this by doubling the evaporation rate, increasing the rainfall coverage of the gridbox from 5% to 30%, and allow the evaporative process to saturate the gridbox (the default model caps the final relative humidity (RH) at 80%). The twin experiment simply inhibits all convective rainfall evaporation. The third experiment detailed attempts to enhance the feedback by increasing the entrainment parameter for shallow and deep convection by a factor of 5, effectively increasing entrainment by a factor of roughly 20.

The effect of inhibiting the rainfall evaporation does not produce an appreciable change in the rainfall organisation in the tropics, while there does appear to be an influence when rainfall evaporation is enhanced, with signs that the convective systems become somewhat longer-lived (not shown). The power of the 200 hPa velocity potential projected onto the two leading EOFs indicates that in the case where rainfall evaporation is suppressed

Name	Experiment
efrm	Default model T_L95
eg3x	Default model T_L159
efv5	Rainfall evaporation inhibited if pressure (P) >800hPa
efv6	Rainfall evaporation enhanced if P>800hPa Evaporation rate doubled, assumed coverage=30% (5%), and no RH limiter applied
efvl	Entrainment rates into convective updraughts increased by 500%
efve	Tropics humidity relaxed to zonal mean on 1 day timescale for P<800hPa
eg4f	Convective parameterization received zonal mean humidity as input for P<800hPa
eg4h	Humidity perturbations about zonal mean are amplified by 3 as input to convective parameterization for P<800hPa
eg44	Entrainment rates into convective updraughts increased by 300% CAPE closure timescale 250s (default=3600s)
efvl	Entrainment rates into convective updraughts increased by 300% convective precipitation efficiency increased by 30%, CAPE closure timescale 450s (default=3600s)
eg2j	Prognostic convective 'memory' implemented such that convective triggering is facilitated in regions previous subject to convective activity

Table 1: Sensitivity experiments to investigate convective water vapour feedback. In all cases the changes are only applied in the Tropics where $|lat| < 20^o$

the propagating mode is enhanced, while amplifying the rainfall evaporation suppresses the MJO-like mode.

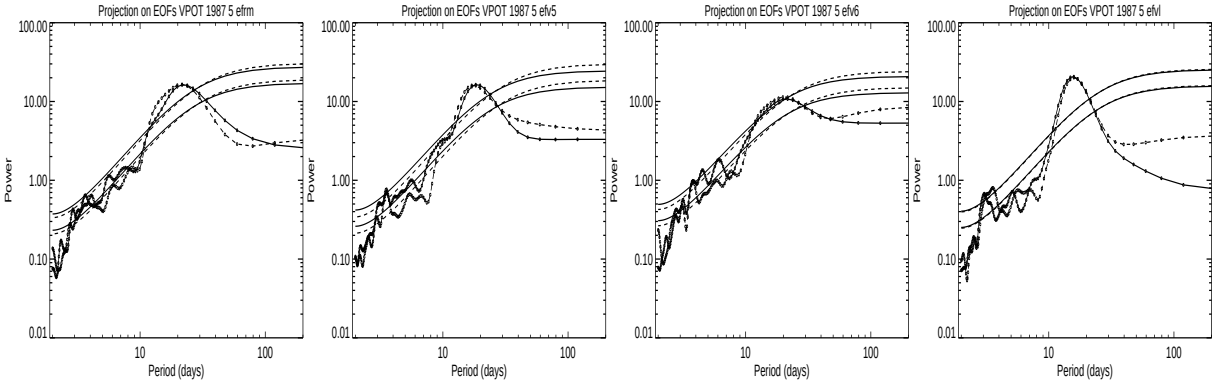

Figure 7: The projection of the 200 hPa VPOT on the EOF 1 (solid) and EOF 2 (dotted). The smooth background lines indicate the 90 and 95% significance levels.

When the entrainment factor is significantly increased, the effect on the model is more dramatic (Fig. 8). Compared the default model it is seen that the convective precipitation is strongly suppressed by this change, and remains so throughout the 365 day integration. This is contrary to expectations. Experience with models that explicitly resolve convective motions suggests that after an external perturbation is applied to a convectively active atmosphere in a state of quasi-equilibrium, which could take the form of a cooling of the lower boundary condition or a change to the microphysics to increase water loading (synonymous to the entrainment experiment conducted here), the convective activity is indeed initially suppressed. This implies that the radiative cooling of the atmosphere acts unopposed. Eventually the cooling will restore the 'effective' value of the convective available potential energy (CAPE) and deep convection will resume, establishing a new equilibrium with a colder mean state (Tompkins and Craig, 1998). This is not the case with the GCM, and convective activity remains permanently suppressed. Instead the large scale dynamics compensates, and most of the precipitation

is produced in the form of gridscale convective events. Examination of the temperature profile four months into the experiments shows that the case with suppressed parameterized deep convective activity is actually warmer than the control case (Fig. 9).

While criticism may be directed at this experiment for its 'extreme' precipitation characteristics, the gross

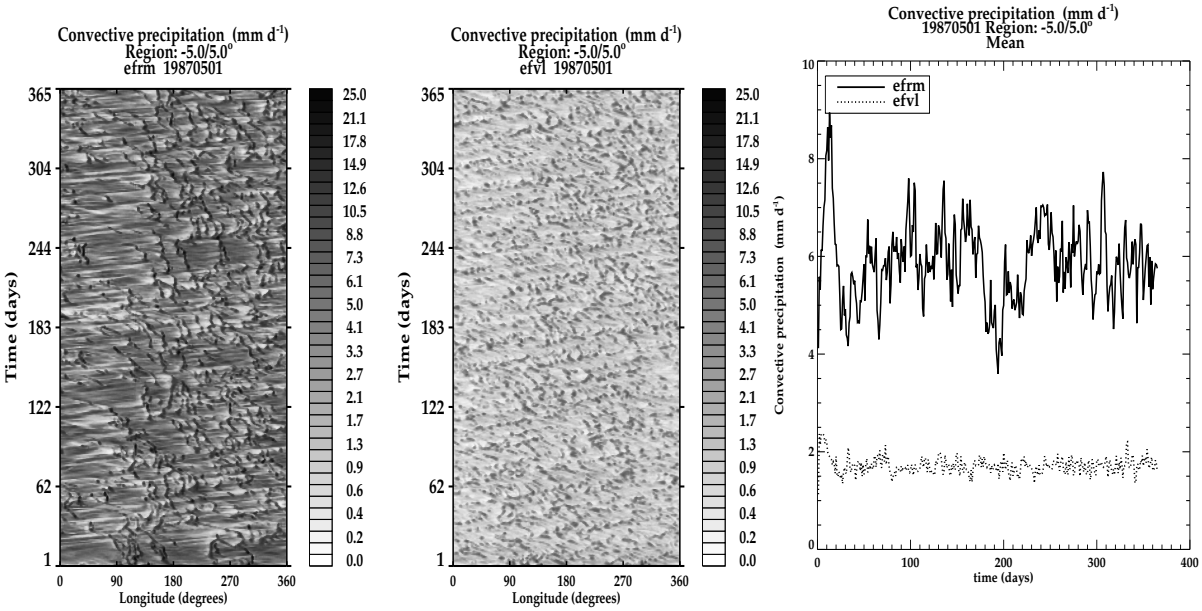

Figure 8: Convective rainfall from the default model (left) and the 5 x entrainment experiment (middle). The right panel shows a time series of the mean convective rainfall to emphasize the difference between the two runs.

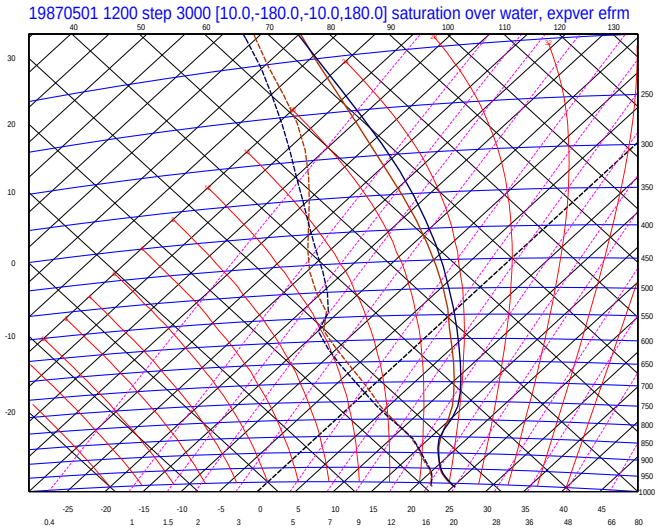

Figure 9: Tephigram showing Tropical mean ($|lat| < 20^o$) temperature and humidity profiles the control experiment (red) and 5 x entrainment experiment (black) at t=4 months

features such as the approximate strength and relative location of the Hadley cell in this aqua planet mode are retained, in contrast to the fourth and fifth experiments of Hayashi and Golder (1997) which completely suppressed all kinetic activity in the upper troposphere. There is thus value in examining the effect the entrainment increase has on the eastward propagating mode. Figure 7 shows that the mode still exists, and indeed is significantly strengthened.

The above result hints that the strength of the propagating mode may in some way be regulated by the balance between the amount of latent heating produced on the gridscale by the cloud condensation scheme with that of the convective parameterization. A surrogate diagnostic for the latent heating balance is provided by examining the ratio of the surface large-scale precipitation (LSP) to the parameterized convective precipitation (CP). The entire cast of sensitivity tests outlined in Table 1 are therefore analysed to contrast the LSP/CP balance with the peak power of the MJO-like mode (Fig. 10). The latter is defined as the peak spectral power of the 200hPa VPOT occurring in the period range of 15 to 80 days between wavenumbers 1 and 3 inclusive. The graph indicates three clear facts. Firstly, since many of the experiments are conducted for two separate years[2], it is evident that for the aqua planet runs the interannual variability in MJO-like peak power is much smaller than the difference between the experiments, justifying the use of only one year of data in the aqua planet framework. Secondly, much more so than the MJO-like power peak, the LSP/CP balance appears to be almost a 'constant' of the model physics, with virtually no variation within integration pairs. Finally, the most striking feature is that there is a clear positive correlation between the power in the eastward propagating mode and the proportion of the rainfall expressed by the large-scale. It should be noted that only the power of the mode is affected. The dominant frequency of the mode does not appear to be significantly influenced.

These results therefore lead to a somewhat unsatisfying conclusion, namely that the zero-order effect of the model alterations are simply to suppress or enhance the amount of parameterized deep convection, altering the balance between the large-scale and parameterized latent heating.

Increasing the proportion of parameterized convection damps the eastward propagating mode, but why should this be the case? One clue is offered when one considers the parameters the large scale and parameterized convection schemes are sensitive to. The deep convection scheme obviously takes the temperature profiles throughout the troposphere into account through its affect on CAPE and the updraught parcel calculation. The dryness of the free troposphere also affects the updraught parcel buoyancy. However, the convective mass flux is dominated by fluctuations in the boundary layer moist static energy (Fillion and Mahfouf, 2003). This contrasts significantly to the latent heating by the large scale cloud scheme. This scheme attempts to parameterize the sources and sinks of cloud water due to a large variety of atmospheric processes (Tiedtke, 1993), but is dominated by convective detrainment, microphysical processes, and in particular the condensation or evaporation of cloud water in rising or subsiding motions. The latter point is pertinent since it implies that the large-scale latent heating is by definition precisely colocated with rising motions, and by association therefore regions of low level convergence. The earlier work on wave-CISK mechanisms for wave instability (e.g. Hayashi, 1970; Lindzen, 1974) were crucially dependent on the use of a Kuo-type convection scheme (Kuo, 1965), which critically constrains convective heating to regions of low level convergence. Using adjustment schemes (e.g. Betts and Miller, 1986) or mass flux schemes (e.g. Tiedtke, 1989) prevents such instabilities.

In a crude sense, we can therefore view the large-scale cloud scheme and the bulk mass-flux convective schemes as effectively competing with each other to represent convective-scale motions, with the former representing convection in a quasi Kuo-type closure. Altering model physics to affect the balance in favour of the large-scale scheme thus possibly amplifies wave motions through a wave-CISK mechanism.

[2]The reader should be reminded that since the boundary SST are fixed and the radiative conditions are set to mean perpetual July in this aqua planet model, then the only difference between the years is the initial conditions

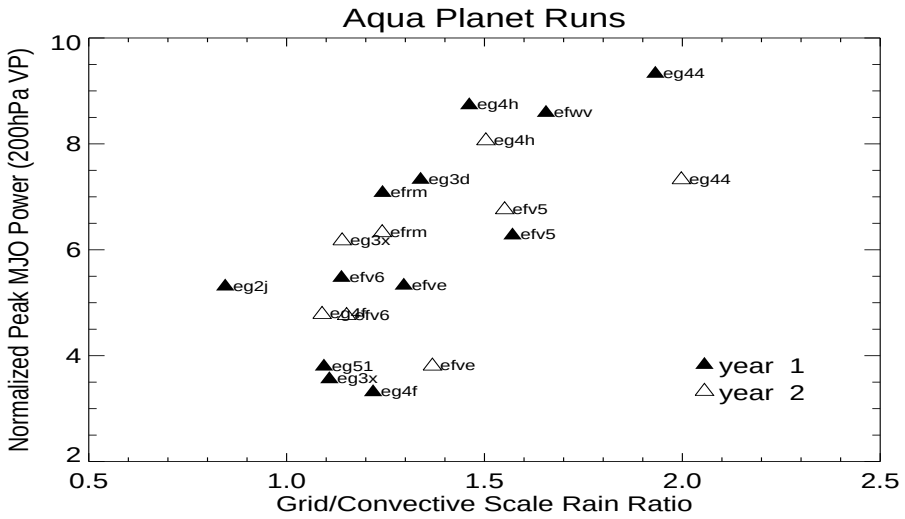

Figure 10: For all experiments the peak MJO-like power is plotted against the ratio of grid scale to parameterized surface precipitation. The peak MJO-like power is defined as the peak power in the 200hPa VPOT spectra between wavenumbers 1 and 3 and a timescale of 15 to 80 days. For some experiments two years are plotted to indicate the level of variability

4 Conclusions

In the ECMWF IFS model a distinct east propagating mode in the lower and upper level zonal wind and 200 hPa velocity potential at wavenumber 1 is identified. With an eastward propagation speed of about 19 m s^{-1} these features are much faster than the MJO signal in observations. More analysis is required, but it is likely that the mode represents moist convectively-coupled Kelvin wave activity.

A significant contrast was noted between the T95 resolution model, used for seasonal forecasting, and higher resolutions such as the T159 model used for the monthly forecast, and the operational T511 model. The higher resolution models appear to significantly damp the low wavenumber modes with respect to analysis data.

The physics of the default model was then modified in a number of ways in an attempt to suppress or exacerbate the feedback between convection and water vapour, to see the consequence for the eastward propagating mode. It was found that the zero-order effect of the model alterations were simply to suppress or enhance the amount of parameterized deep convection, altering the balance between the large-scale and parameterized latent heating. Increasing the proportion of parameterized convection damps the eastward propagating mode. This was consistent with the resolution sensitivity of the default model, for which the T95 version has a different balance in favour of large-scale precipitation, the reasons for which are yet to be ascertained.

It is suggested that because the large-scale latent heating is constrained to occur in regions of upward motion, it could amplify waves through the wave-CISK mechanism, which is irrelevant if bulk mass flux or adjustment convective schemes instead present convective activity in the tropics. Affecting the model balance in a way that suppresses the parameterized convection therefore exacerbates the eastward propagating mode. It is important to stress that it is not our view that this is necessarily beneficial; it is likely that the eastward propagating mode has little in common with the MJO phenomenom in nature and is more probably a convectively forced Kelvin wave response. The findings of this study highlight the danger of resorting automatically to physically-based but nevertheless unsubstantiated hypotheses when working with complex numerical models. It is always tempting to associate model behaviour with mechanisms that one can imagine applying in nature, while in fact numerical artifacts can be dominating a response. The investigation also identify some characteristics of parameterized convection that can be further investigated, such as its relation to large-scale motions for example.

Acknowledgements

Nils Wedi, Pedro Viterbo and Mariano Hortal are all thanked for their technical help with the ECMWF model. Andrew Gregory and Pete Inness provided the wavenumber-frequency code used to create Fig. 10.

References

Barnett, T. P., K. Hasselmann, M. Chelliah, T. Delworth, G. Hegerl, P. Jones, E. Rasmussen, E. Roeckner, C. Ropelski, B. Santer, and S. Tett, 1999: Detection and attribution of recent climate change: A status report, *Bull. Amer. Meteor. Soc.*, **80**, 2631–2659.

Betts, A. K. and M. J. Miller, 1986: A new convective adjustment scheme: Part 2: Single column tests using GATE WAVE, BOMEX, ATEX and arctic air-mass data sets, *Q. J. R. Meteorol. Soc.*, **112**, 693–709.

Bladé, I. and D. L. Hartmann, 1993: Tropical intraseasonal oscillations in a simple nonlinear model, *J. Atmos. Sci.*, **50**, 2922–2939.

Emanuel, K. A., 1987: An air-sea interaction model of intraseasonal oscillations in the tropics, *J. Atmos. Sci.*, **44**, 2324–2340.

Emanuel, K. A., 1991: A scheme for representing cumulus convection in large-scale models, *J. Atmos. Sci.*, **48**, 2313–2335.

Esbensen, S., 1978: Bulk thermodynamic effects and properties of small tropical cumuli, *J. Atmos. Sci.*, **35**, 826–831.

Fillion, L. and J.-F. Mahfouf, 2003: Jacobians of an operational prognostic cloud scheme, *Mon. Wea. Rev.*, **131**, 2838–2856.

Grabowski, W. W., 2003: MJO-like coherent structures: Sensitivity simulations using the cloud-resolving convection parameterization (CRCP), *J. Atmos. Sci.*, **60**, 847–864.

Grabowski, W. W. and M. W. Moncrieff, 2004: Moisture-convection feedback in the Tropics, *Q. J. R. Meteorol. Soc.*, **130**, submitted.

Hayashi, Y., 1970: A theory of large-scale equatorial waves generated by condensation heat and accelerating the zonal wind, *J. Meteor. Soc. of Japan*, **48**, 140–160.

Hayashi, Y. and D. G. Golder, 1997: United mechanisms for the generation of low- and high-frequency tropical waves. Part I: Control experiments with moist convective adjustment, *J. Atmos. Sci.*, **54**, 1262–1276.

Hendon, H. H., 2000: Impact of air-sea coupling on the Madden-Julian oscillation in a general circulation model, *J. Atmos. Sci.*, **57**, 3939–3952.

Inness, P. M. and J. M. Slingo, 2003: Simulation of the Madden-Julian oscillation in a coupled general circulation model. Part I: Comparison with observations and an atmosphere-only GCM, *J. Climate*, **16**, 345–364.

Inness, P. M., J. M. Slingo, S. J. Woolnough, R. B. Neale, and V. D. Pope, 2001: Organization of tropical convection in a GCM with varying vertical resolution; implications of the Madden-Julian Oscillation, *Climate Dynamics*, **17**, 777–793.

Jenkins, G. M. and D. G. Watts, 1968: *Spectral analysis and its application*, Holden-Day, 525 pp.

Jung, T. and A. M. Tompkins, 2003: Systematic errors in the ECMWF forecasting system, Technical Report 422, European Centre for Medium-Range Weather Forecasts, Shinfield Park, Reading RG2 9AX, U.K., pp72.

Kuo, H.-L., 1965: On formation and intensification of the tropical cyclones through latent heat release by cumulus convection, *J. Atmos. Sci.*, **22**, 40–63.

Lee, M. I., I. S. Kang, J. K. Kim, and B. E. Mapes, 2001: Influence of cloud-radiation interaction on simulating tropical intraseasonal oscillation with an atmospheric general circulation model, *J. Geophy. Res.*, **106**, 14219–14233.

LeMone, M. A. and E. J. Zipser, 1980: Cumulonimbus vertical velocity events in GATE. Part I: Diameter, intensity and mass flux., *J. Atmos. Sci.*, **37**, 2444–2457.

Lindzen, R. S., 1974: Wave-CISK in the Tropics, *J. Atmos. Sci.*, **31**, 156–179.

Madden, R. A. and P. R. Julian, 1971: Detection of a 40-50 day oscillation in the zonal wind in the tropical pacific, *J. Atmos. Sci.*, **5**, 702–708.

Madden, R. A. and P. R. Julian, 1972: Description of global-scale circulation cells in the tropics with a 40-50 day period, *J. Atmos. Sci.*, **6**, 1109–1123.

Neale, R. B. and B. J. Hoskins, 2000: A standard test for AGCMs and their physical parameterizations. I: The proposal, *Atmos. Sci. Letters*, **1**, 101–107.

Neelin, J. D., I. M. Held, and K. H. Cook, 1987: Evaporation-wind feedback and low-frequency variability in the tropical atmosphere, *J. Atmos. Sci.*, **44**, 2341–2348.

Nicholls, S. and M. A. Lemone, 1980: The fair weather boundary-layer in GATE - The relationship of sub-cloud fluxes and structure to the distribution and enhancement of cumulus clouds, *J. Atmos. Sci.*, **37**, 2051–2067.

Randall, D. A. and G. J. Huffman, 1980: A stochastic model of cumulus clumping, *J. Atmos. Sci.*, **37**, 2068–2078.

Raymond, D. J., 2001: A new model of the Madden Julian Oscillaton, *J. Atmos. Sci.*, **58**, 2807–2819.

Slingo, J. M., K. R. Sperber, J. S. Boyle, J. P. Ceron, M. Dix, B. Dugas, W. Ebisuzaki, J. Fyfe, D. Gregory, J. F. Gueremy, J. Hack, A. Harzallah, P. Inness, A. Kitoh, W. K. M. Lau, B. McAvaney, R. Madden, A. Matthews, T. N. Palmer, C. K. Park, D. Randall, and N. Renno, 1996: Intraseasonal oscillations in 15 atmospheric general circulation models: Results from an AMIP diagnostic subproject, *Clim. Dyn.*, **12**, 325–357.

Tiedtke, M., 1989: A comprehensive mass flux scheme for cumulus parameterization in large-scale models., *Mon. Wea. Rev.*, **117**, 1779–1800.

Tiedtke, M., 1993: Representation of clouds in large-scale models, *Mon. Wea. Rev.*, **121**, 3040–3061.

Tompkins, A. M., 2001: Organization of tropical convection in low vertical wind shears: The role of water vapor, *J. Atmos. Sci.*, **58**, 529–545.

Tompkins, A. M. and G. C. Craig, 1998: Time-scales of adjustment to radiative-convective equilibrium in the tropical atmosphere, *Q. J. R. Meteorol. Soc.*, **124**, 2693–2713.

Vitart, F., M. A. Balmaseda, L. Ferranti, and D. Anderson, 2003: Westerly wind events and the 1997/98 El Nino event in the ECMWF seasonal forecasting system: A case study, *J. Climate*, **16**, 3153–3170.

von Storch, H. and F. W. Zwiers, 1999: *Statistical Analysis in Climate Research*, Cambridge University Press, 484 pp.

Woolnough, S. J., J. M. Slingo, and B. J. Hoskins, 2001: The organisation of tropical convection by intraseasonal sea surface temperature anomalies, *Q. J. R. Meteorol. Soc.*, **127**, 887–907.

Zhang, C. D. and P. J. Webster, 1992: Laterally forced equatorial perturbations in a linear-model. Part 1: stationary transient forcing, *J. Atmos. Sci.*, **49**, 585–607.